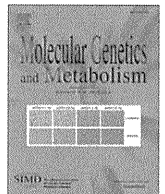




Contents lists available at SciVerse ScienceDirect

Molecular Genetics and Metabolism

journal homepage: www.elsevier.com/locate/ymgme

Effect of curcumin in a mouse model of Pelizaeus–Merzbacher disease

Li-Hua Yu^a, Toshifumi Morimura^a, Yurika Numata^a, Ryoko Yamamoto^a, Naoko Inoue^a, Barbara Antalffy^b, Yu-ichi Goto^a, Kimiko Deguchi^{a,c}, Hitoshi Osaka^d, Ken Inoue^{a,*}^a Department of Mental Retardation and Birth Defect Research, National Institute of Neuroscience, National Center of Neurology and Psychiatry, Kodaira, Japan^b Department of Pathology, Texas Children's Hospital, Houston, USA^c Department of Pediatric Neurology, Baylor College of Medicine, Houston, USA^d Division of Neurology, Clinical Research Institute, Kanagawa Children's Medical Center, Yokohama, Japan

ARTICLE INFO

Article history:

Received 24 February 2012

Accepted 24 February 2012

Available online xxxx

Keywords:

Treatment

Protein misfolding

Hypomyelinating disease

CNS

Food compound

Model mouse

ABSTRACT

PLP1 amino acid substitutions cause accumulation of misfolded protein and induce endoplasmic reticulum (ER) stress, causing Pelizaeus–Merzbacher disease (PMD), a hypomyelinating disorder of the central nerve system. Currently no effective therapy is available for PMD. Promoted by its curative effects in other genetic disease models caused by similar molecular mechanisms, we tested if curcumin, a dietary compound, can rescue the lethal phenotype of a PMD mouse model (*myelin synthesis deficient*, *msd*). Curcumin was administered orally to *myelin synthesis deficient* (*msd*) mice at 180 mg·kg⁻¹·day⁻¹ from the postnatal day 3. We evaluated general and motor status, changes in myelination and apoptosis of oligodendrocytes by neuropathological and biochemical examination, and transcription levels for ER-related molecules. We also examined the pharmacological effect of curcumin in cell culture system. Oral curcumin treatment resulted in 25% longer survival ($p < 0.01$). In addition, oligodendrocytes undergoing apoptosis were reduced in number ($p < 0.05$). However, no apparent improvement in motor function, neurological phenotype, and myelin formation was observed. Curcumin treatment did not change the expression of ER stress markers and subcellular localization of the mutant protein *in vitro* and/or *in vivo*. Curcumin partially mitigated the clinical and pathological phenotype of *msd* mice, although molecular mechanisms underlying this curative effect are yet undetermined. Nonetheless, curcumin may serve as a potential therapeutic compound for PMD caused by *PLP1* point mutations.

© 2012 Elsevier Inc. All rights reserved.

1. Introduction

Pelizaeus–Merzbacher disease (PMD) is a devastating X-linked neurodevelopmental disease characterized by a failure of myelination in the central nervous system (CNS) [1,2]. Clinical symptoms of PMD include nystagmus, spastic quadriplegia, ataxia, dystonia, and developmental delay. Mutations in the proteolipid protein gene (*PLP1*), encoding a major myelin membrane protein, are responsible for PMD [3]. *PLP1* mutations include genomic duplication, deletion, and point mutations, each of which leads to CNS dysmyelination through distinct molecular mechanisms [1,2]. Despite all that is known about PMD, no effective therapy has been established to date. *PLP1* point mutations, many of which lead to amino acid substitutions, cause improper folding and accumulation of the mutant proteins in the endoplasmic reticulum (ER), resulting in disruption of ER homeostasis and induction of apoptosis of oligodendrocytes mediated by unfolded protein response (UPR) [4,5]. Thus, modulation of this pathological process may mitigate the manifestation of PMD.

* Corresponding author at: Department of Mental Retardation and Birth Defect Research, National Institute of Neuroscience, National Center of Neurology and Psychiatry, 4-1-1 Ogawahigashi, Kodaira, Tokyo 187-8502, Japan. Fax: +81 423461743.

E-mail address: kinoue@ncnp.go.jp (K. Inoue).

Recently, curcumin (diferuloylmethane), a polyphenol dietary compound derived from the curry spice turmeric, has been used in several therapeutic strategies to rescue rodent models from genetic diseases caused by mutations that lead to protein misfolding. Four genes responsible for 3 major genetic disorders, *CFTR* (cystic fibrosis; CF), *MPZ* and *PMP22* (Charcot-Marie-Tooth disease type 1; CMT1), and *RHO* (retinitis pigmentosa), have been targeted by this treatment both *in vitro* and *in vivo*, and improvements in cellular and clinical phenotypes have been reported [6–9]. These findings implicated that curcumin ameliorates the phenotypes of protein misfolding diseases, including PMD. In this study, we examined the therapeutic effect of oral curcumin administration in a PMD model mouse, *myelin synthesis deficient* (*msd*), carrying a spontaneous A242V missense mutation in the *PLP1* gene.

2. Materials and methods

2.1. Ethical statement

All animals were maintained and utilized in the study according to the institutional guidelines of the National Center for Neurology and

Psychiatry animal care committee and approval of all experimental protocols (2011018).

2.2. Animals, treatment, and phenotypic evaluation

Msd mice [10] were maintained on a B6C3F1/J background. Wild-type male littermates served as controls. In each cage, 6 newborn mice and their mother were housed until the weaning at 1 month after birth, considering the delayed growth of the *msd* mice. Treated and untreated groups were separated by cage. Curcumin (Sigma, C7727) was dissolved in commercially available milk for rodents (10 mg/ml), and was orally administered via a micropipette 6 days/week at 180 mg/kg/day starting at P3. We determined the amount of curcumin according to the previous studies in mice and humans. The same amount of milk was given to the untreated mice. High bio-availability of curcumin in the brain was shown [8]. Essentially, all evaluations were performed in a blinded fashion. The wire hanging test was utilized to evaluate motor performance [11]. Mice were placed on a wire mesh, which was then inverted; latency to fall was recorded. Each mouse was tested 3 times with a 10-min interval between the tests.

2.3. Neuropathological analyses

Mouse brains were fixed with 4% paraformaldehyde in phosphate buffered saline (PBS) and embedded in paraffin using a standard protocol. Coronal serial sections (6 mm thick) around Bregma P1.4 mm were subjected to immunostaining using the following antibodies: mouse anti-myelin basic protein (MBP, SMI99, 1:1000, Covance), rabbit anti-active Caspase3 (#9661, 1:400, Cell Signaling), mouse anti-2',3'-cyclic nucleotide 3'-phosphodiesterase (CNPase, SMI91, 1:500, Covance), mouse anti-gial fibrillary acidic protein (GFAP, MAB3402 1:1000, Chemicon), and mouse anti-neuronal nuclei (NeuN, A60, 1:1000, Chemicon). For the Terminal deoxynucleotidyl transferase dUTP nick end labeling (TUNEL) assay, we utilized the ApopTag Peroxidase In Situ Apoptosis Detection Kit (Chemicon). For the bright field signal detection, we used biotinylated secondary antibody and peroxidase-conjugated avidin-biotin complex (VECTASTAIN Elite ABC kit, Vector Laboratories) with either ImmPACT DAB or NovaRED (Vector Laboratories). For the fluorescent double staining, Alexa fluor-conjugated secondary antibodies (Molecular Probes) were used followed by visualization using the FLUOVIEW Laser scanning microscope (Olympus).

2.4. Quantification of MBP by enzyme-linked immunosorbent assay (ELISA)

Brains were obtained from treated or untreated *msd* and wild-type mice at P21 (3 animals for each group). A 2-mm-thick coronal slice around Bregma P1.4 mm was sonicated in lysis buffer (20 mM Tris-HCl, pH 6.8, 1% SDS, 4 mM EDTA), followed by centrifugation at 12,000 rpm for 30 min to obtain supernatants. Standard sandwich ELISA was utilized for the MBP measurement using mouse anti-MBP antibody (1:1000, Covance) for coating the microtiter plates and rabbit anti-MBP antibody (1:1000, Dako) for detection using SureBlue Reserve TMB Microwell Peroxidase substrate (KPL). Protein concentrations were determined by measurements at 450 nm using a plate reader (1420 Multilabel Counter, Perkin Elmer). The measurement was repeated 4 times for each animal.

2.5. Electron microscopic analysis of the optic nerve

Optic nerves were isolated and fixed in 2% glutaraldehyde and 2% paraformaldehyde in 0.1 M PBS (pH 7.4), followed by postfixation in 1% osmium (OsO₄) in PBS. After serial dehydration, the optic nerves were flat-embedded in Epon. Serial ultrathin sections cut at 70 nm were examined under an electron microscope (model H-600, Hitachi). Semi-thin

sections cut at 1 mm were stained with toluidine blue and examined under a bright field microscope for quantification of myelinated fibers.

2.6. Quantitative reverse transcriptase (RT)-PCR

We isolated internal capsule (IC) from sliced fresh brains (3 animals for each group) by punching the IC out using a chopped micropipette tip. Total RNA was extracted from the IC and spinal cords using RNeasy Protect Mini Kit (Qiagen) and was converted to cDNA using Superscript III reverse transcriptase and random primers (Invitrogen). We determined the transcript levels for the genes listed below using pre-designed TaqMan probes (Applied Biosystems) and synthesized cDNA as templates for quantitative RT-PCR (7900HT, Applied Biosystems). The assay IDs for the specific genes were: *Grp78/Bip*: Mm00517691, *Herpud1*: Mm00445600, *calnexin*: Mm00500330, *calreticulin*: Mm00482936, *Chop*: Mm00492097, *Gadd45a*: Mm00432802, *Actb*: Mm00607939. Relative measurement to *Actb* was calculated using the DDCT method following the manufacturer's standard protocol.

2.7. Cell culture and in vitro expression studies

Human *PLP1* cDNA, either wild-type or A242V mutant, was cloned into a strong mammalian expression vector, pCAG, under cytomegalovirus and actin promoters and fused with the FLAG tag to the carboxyl terminus of PLP1 to generate pCAG-PLP1wt-FLAG and pCAG-PLP1msd-FLAG. HeLa cells (originally obtained from ATCC; cat# CCL-2), maintained in DMEM with 10% FBS, were transfected with 2 mg of plasmid DNA using TransIt LT1 (Mirus). Twenty-four hours later, cells were treated with curcumin (10 mg/ml in DMSO) or vehicle (DMSO) for 6 h at various concentrations and harvested for the extraction of total RNA, which was then converted to cDNA. We determined the expression level of the same 6 genes associated with unfolded protein response (UPR) along with *GAPDH* as a control, using human pre-designed TaqMan probes (Applied Biosystems).

HeLa cells treated with curcumin for 12 h were transfected with pCAG-PLP1msd-FLAG. After 24 h of incubation, cell surface proteins were biotinylated as described elsewhere [12]. Cells were harvested with streptavidin beads (Pierce) to isolate the plasma membrane fraction. Similarly, cells were treated with 0.01% digitonin to obtain the plasma membrane and cytosolic fractions. After the collection of the supernatant, cells were harvested with 1% Triton and 0.1% SDS to obtain the organelle and nuclear fractions. Protein extracts from each fraction were used for western blotting with mouse anti-FLAG antibody (Sigma, M2, 0.5 mg/ml).

HeLa cells transfected with pCAG-PLP1wt-FLAG and pCAG-PLP1msd-FLAG were fixed with 4% paraformaldehyde and subjected to fluorescent immunocytochemistry with double labeling using the mouse anti-FLAG and rabbit anti-calnexin (Enzo, ADI-SPA-860, 1:200) antibodies, followed by visualization with a confocal laser microscope (FV-1000, Olympus).

2.8. Statistical analyses

For survival analysis (Fig. 1A), we used Kaplan–Meier method combined with a generalized Wilcoxon test. For the motor function analysis (Fig. 1C), we used one-way analysis of variance (ANOVA) and Student's *t*-test. For the ELISA (Fig. 2B), we used a repeated measures analysis of variance using the residual maximum likelihood (REML). For the quantification of myelin fibers (Fig. 2D), we used one-way ANOVA and Student's *t*-test. For the TUNEL and caspase3 assays (Figs. 3 and 4), we used a repeated measures analysis of variance using the REML. For the quantitative RT-PCR analyses (Fig. 5 and Fig S1), we used one-way ANOVA and Student's *t*-test. Mainly, means ± standard deviations were shown in the figures. All statistical examination was carried out using JMP software (SAS Institute).

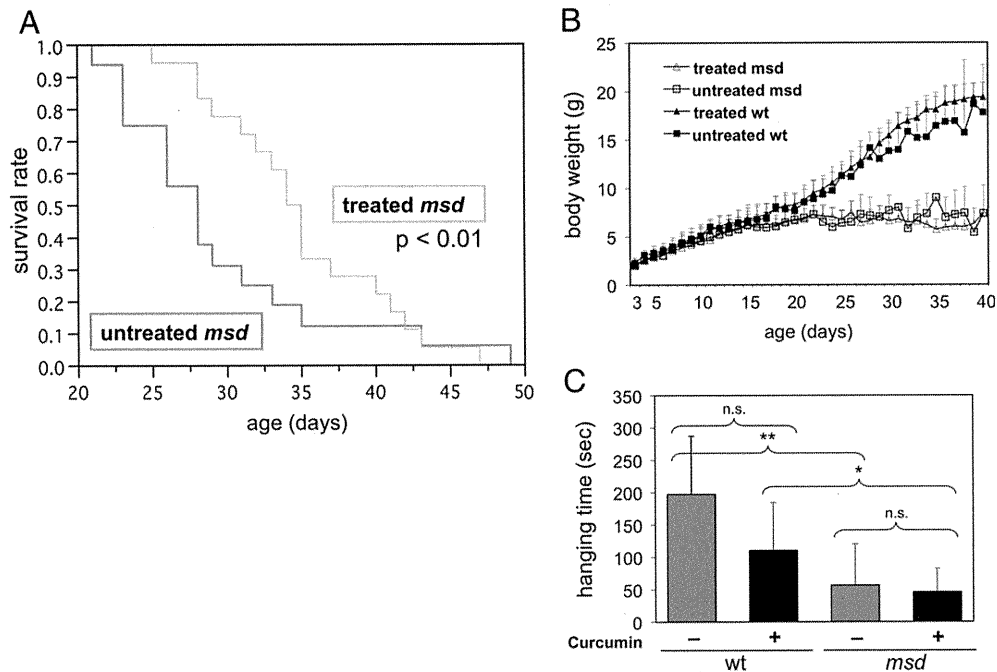


Fig. 1. Effect of curcumin on the lifespan, growth curve and motor performance of *msd* mice. A. Survival curves of treated *msd* mice ($n = 18$, green) and untreated mice ($n = 16$, red). The life spans of treated mice were statistically longer than those of untreated mice. Data from wild-type mice were not shown because no mouse died during the course of the study regardless of treatment. B. Body weight changes are shown for treated *msd* (open triangle, $n = 41$), untreated *msd* (open square, $n = 17$), treated wild-type (closed triangle, $n = 35$) and untreated wild-type (open square, $n = 17$) mice. *Msd* mice showed growth retardation from 3 weeks of age; curcumin treatment had no effect on this growth retardation. The data are presented as mean \pm SD. C. Motor function was evaluated by the wire hanging test. The data are presented as mean \pm SD. Untreated wild-type (left gray bar: $n = 5$); treated wild-type (left filled bar: $n = 4$); untreated *msd* (right gray bar: $n = 10$); and treated *msd* (right filled bar: $n = 11$). Statistical significances are shown as asterisks: * $p < 0.05$; ** $p < 0.01$. n.s. = not significant. *Msd* mice fell significantly earlier than wild-type mice regardless of treatment. No significant difference was observed between treated and untreated *msd* mice.

194 3. Results

195 3.1. Curcumin extended the lifespan of *msd* mice

196 All experiments were performed in 4 groups of male mice: treated
197 or untreated *msd* mice, and treated or untreated wild-type mice. In

general, neurological symptoms of *msd* mice initiated at postnatal 198
day 7 (P7) with moderate tremors, which gradually worsened, fol- 199
lowed by dystonia occurring around P21. All *msd* mice died within 200
2 months due to prolonged severe dystonic cramps, which resulted 201
in respiratory failure. When treated with curcumin, *msd* mice lived 202
for a median of 35 days (ranging from 25 to 47 days, Fig. 1A), which 203

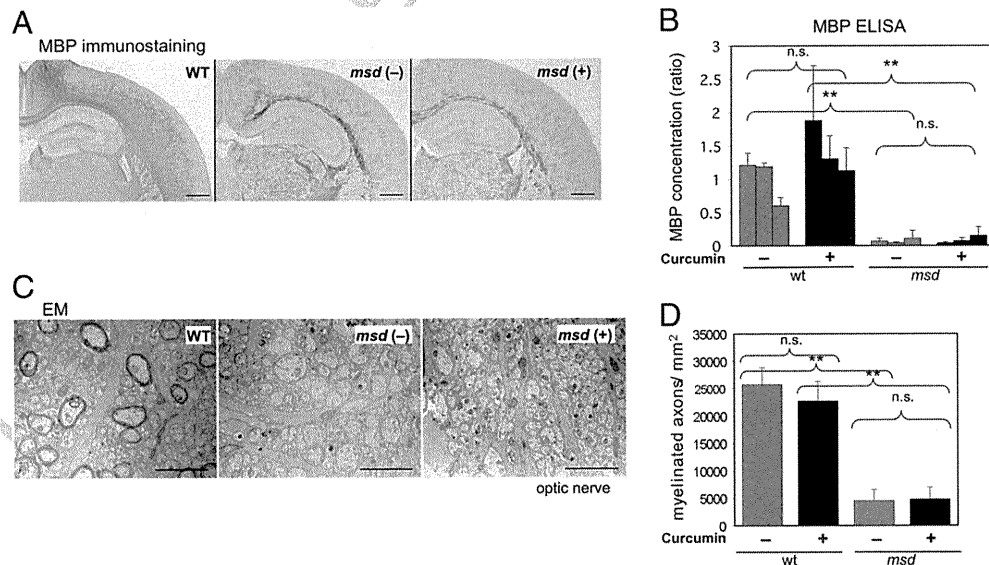


Fig. 2. Curcumin did not ameliorate CNS dysmyelination. A. Coronal sections of P21 mouse brains with MBP immunostaining are shown. Both treated and untreated *msd* brains (*msd* (-) and *msd* (+), respectively) showed sparse and weak staining in the white matter and cortex in comparison with the untreated wild-type brains (WT). All slides were stained simultaneously to avoid variation in staining due to the difference in wash and incubation times. Scale bars show 500 μ m. B. Quantification of MBP in isolated IC by ELISA at P21 ($n = 3$). Relative amounts to the average of untreated wild-type mice are shown. Note that *msd* mice, regardless of treatment, showed extremely low amounts of MBP and the treatment did not change the protein expression level. The data are presented as mean \pm SD. C. Coronal sections of optic nerves examined by electron microscopy at P14 are shown in the same order as A. In comparison with untreated wild-type mice, both treated and untreated *msd* mice optic nerves barely exhibited myelinated axons. Scale bar shows 2 μ m. No apparent improvement by curcumin treatment was observed at P21 and P28 (data not shown). D. Number of myelin fibers in optic nerves was counted using the same specimen as C stained with toluidine blue ($n = 3$ in each group). Treated and untreated *msd* mice showed no significant difference in the number of myelinated fibers, which were significantly fewer than in wild-type mice. The data are presented as mean \pm SD. Statistical significances are shown as asterisks: * $p < 0.05$; ** $p < 0.01$; n.s. = not significant.

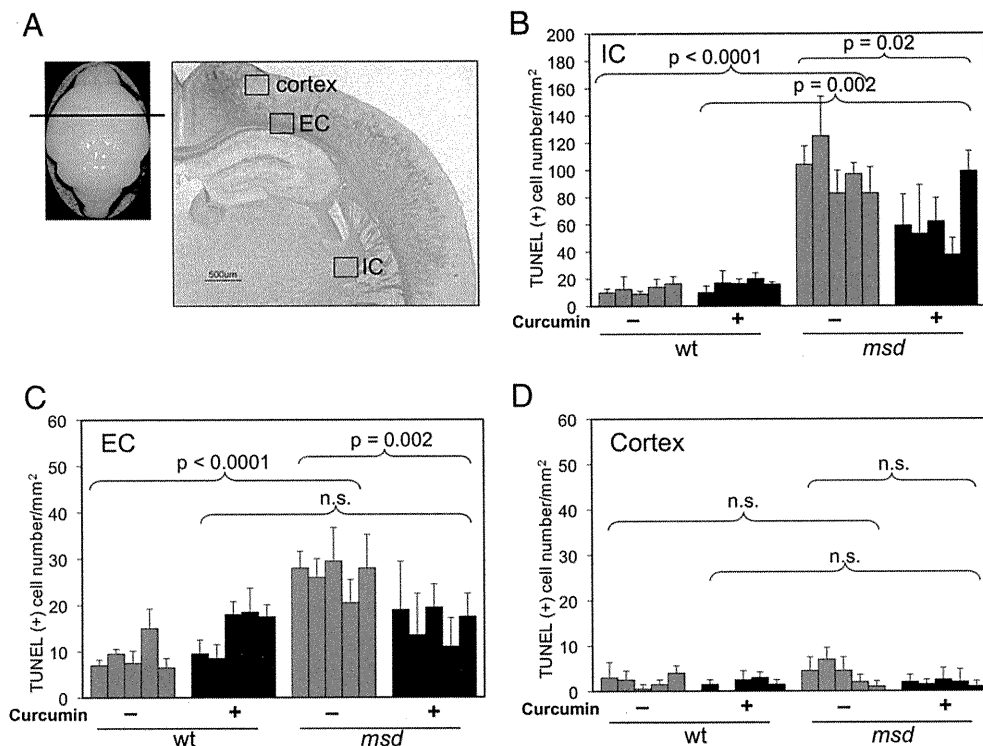


Fig. 3. Quantification of TUNEL-positive apoptotic cells. A. P21 mouse brain showing the position of examination (left; horizontal bar). Coronal section of P21 wild-type mouse brain shows the areas of examination (right; boxes). B–D. TUNEL-positive cells were microscopically counted in the white matter (internal capsule, IC; external capsule; EC) and the parietal cortex (M1 and M2 area) at P21 under a bright field microscope at 100-fold magnification. Each bar represents an averaged TUNEL-positive cell number per mm² (4 fields examined) in each mouse. The data were presented as mean \pm SD. Both in the IC (B) and EC (C), untreated *msd* mice showed enhanced apoptosis. Treated *msd* mice showed significantly fewer number of TUNEL-positive cells than untreated *msd* mice. In the EC of the treated *msd*, apoptotic cell number was reduced to the level of wild-type mice. Untreated wild-type (gray bars: n = 5); treated wild-type (blue bars: n = 5); untreated *msd* (red bars: n = 5); treated *msd* (green bars: n = 5) mice. n.s. = not significant.

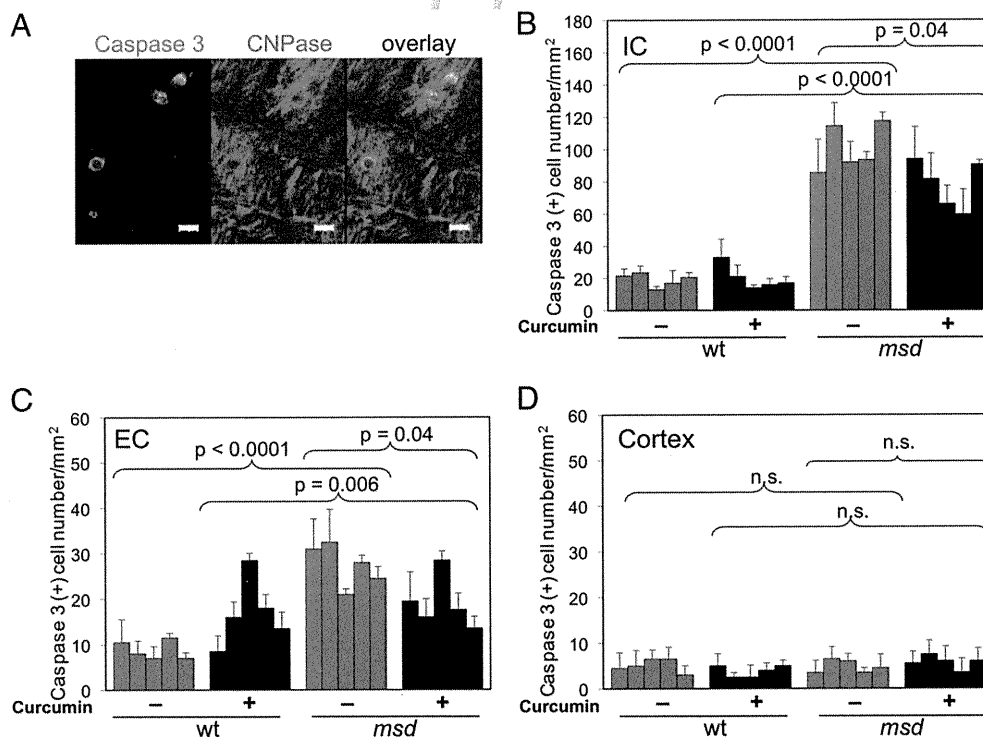


Fig. 4. Quantification of active caspase3-positive apoptotic cells by immunohistochemistry. A. Fluorescent double staining of active caspase3 (left; green) and CNPase (middle; red) visualized by confocal microscopy demonstrated cytoplasmic overlapping signals (right; overlay) (scale bar shows 100 μ m). Note that detection of cytoplasmic staining of CNPase required an overexposure of myelin sheath staining. B–D. Active caspase3-positive cells were quantified in the white matter (IC and EC) and the parietal cortex in P21 mice. The experimental design was same as the TUNEL assay demonstrated in Fig. 2. In the IC and EC (but not the cortex), untreated *msd* mice showed enhanced apoptosis. Treated *msd* mice showed significantly fewer numbers of caspase3-positive cells than untreated *msd* mice. The data are presented as mean \pm SD. n.s. = not significant.

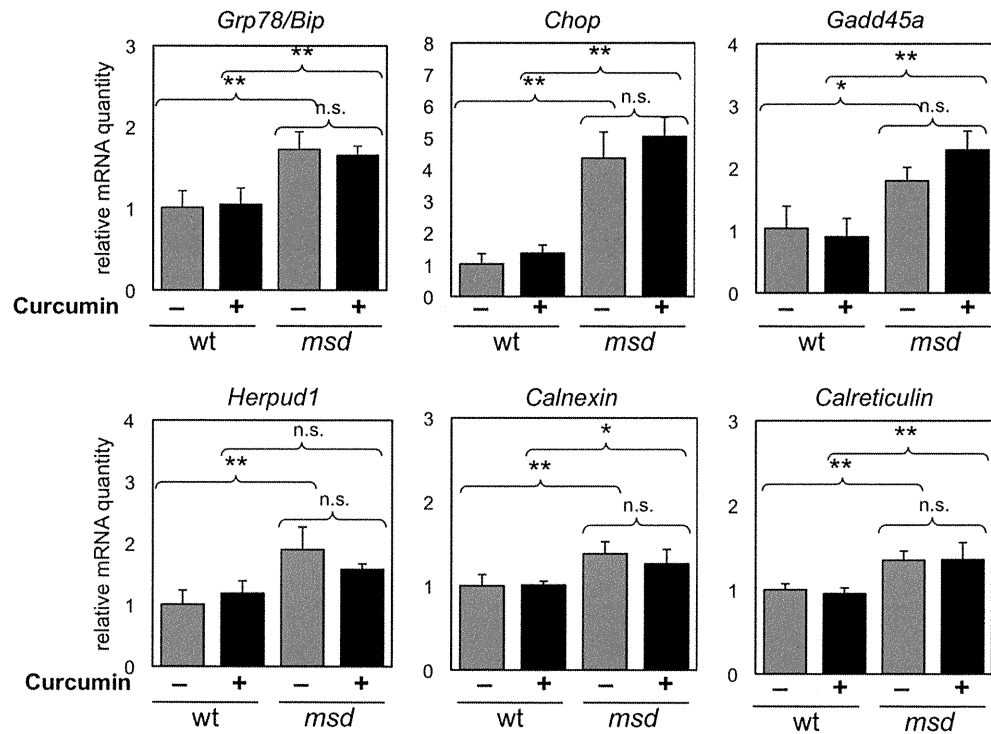


Fig. 5. Quantitative RT-PCR analyses for genes associated with UPR in *msd* mice. Expression levels for *Grp78/Bip*, *Chop*, *Gadd45a*, *Herpud1*, *calnexin*, and *calreticulin* were determined in the isolated IC at P14. *Gapdh* was used as an inner control. Each column represents untreated wild-type ($n=3$, gray bar), treated wild-type ($n=3$, blue bar), untreated *msd* ($n=3$, red bar), and treated *msd* ($n=3$, green bar) mice. Ratios to untreated wild-type mice are shown. The data are presented as mean \pm SD. Statistical significances are shown as asterisks: * $p < 0.05$; ** $p < 0.01$; n.s. = not significant.

was 7 days longer than the untreated *msd* mice (median of 28 days ranging from 21 to 49 days, $p < 0.01$). Curcumin had no effect on the survival of wild-type mice.

Besides the ~25% longer survival, difference in neurological phenotypes between treated and untreated mice, including onset and severity of tremor, gait disturbance, and frequency and severity of dystonic cramping, was not obvious by observation. Additionally, no difference was noted in the growth curve and motor function as determined by the wire hanging test between treated and untreated *msd* mice (Figs. 1B and C).

3.2. Curcumin did not ameliorate CNS dysmyelination

Given the effects of curcumin on survival of *msd* mice, we then determined if this beneficial effect of curcumin could further ameliorate dysmyelination in the CNS. First, we examined the expression of myelin basic protein (MBP), a major component of the mature myelin sheath, to evaluate myelin formation by immunohistochemistry (Fig. 2A). Based on the MBP expression profile determined in wild-type mice, we decided to evaluate myelin formation at P21. In the white matter (IC and external capsule (EC), respectively) of the untreated *msd* brains, MBP-positive myelin fibers were present sparsely and weakly when compared to wild-type mice. Treated *msd* mice also showed similarly sparse MBP-positive myelin fibers, which was essentially indistinguishable from untreated mice.

Next, we measured the MBP protein level using ELISA (Fig. 2B). In wild-type mice, MBP protein increased more than twice from P14 to P21, representing a progression of myelination (P14 data not shown). Untreated *msd* mice showed only ~5 to 10% amount of wild-type mice at P21, consistent with the findings in immunohistochemistry. We observed no significant increase in the amount of MBP for treated *msd* mice both at P14 and P21, also confirming the immunohistochemistry findings.

In addition, we examined the ultrastructure of the myelin sheath by electron microscopic analysis of optic nerves at P21 (Fig. 2C).

While myelin ensheathment was apparent around large axons in wild-type mice, almost no myelin was observed in untreated *msd* mice. Similarly, treated *msd* mice showed only unmyelinated axons. We also quantified the number of myelinated axons in toluidine blue-stained sections and found that treated and untreated *msd* mice both showed similarly reduced number of myelinated fibers (Fig. 2D). Altogether, curcumin did not ameliorate dysmyelination in *msd* mice and the extended lifespan was unlikely to be the result of improvement in myelination.

3.3. Curcumin mitigated apoptosis of oligodendrocytes

Next, we examined the effect of curcumin on the apoptotic cell death of oligodendrocytes at P21. In *msd* mice, TUNEL- and caspase 3-positive apoptotic cells were increased in the white matter (IC and EC) where oligodendrocytes predominate the cell population, but were not in the cortex (Figs. 3 and 4). A double-labeling study showed that the vast majority of either TUNEL- or caspase3-positive cells were also positive for CNPase, but were barely positive for GFAP or NeuN (Fig. 4A, Table 1). These findings suggest that cells undergoing apoptosis in the white matter of the *msd* brains are predominantly oligodendrocytes [4].

Upon curcumin administration, the treated *msd* mice showed significant decreases in the number of TUNEL-positive apoptotic cells in the white matter compared to the untreated mice (Fig. 3). No such change was observed in the wild-type mice. We also observed similar findings in active caspase3-positive cells both in the IC and EC (Figs. 4B–D). These results suggest that curcumin can mitigate the apoptotic cell death of oligodendrocytes in the *msd* mouse brain.

3.4. Effects of curcumin on the expression of UPR markers and the subcellular localization of mutant PLP1 protein

Next, we determined if curcumin could change the expression of genes associated with UPR, as observed in retinitis pigmentosa study

Table 1
Double labeling studies with cell-specific markers and TUNEL or active caspase3.

Cell-specific markers	Number of double (+) cells/ TUNEL(+) cells (%)			Number of double (+) cells/ caspase3(+) cells (%)		
	Cortex	IC ^c	EC ^d	Cortex	IC ^a	EC ^b
CNPase	7/ 7(100)	226/ 226(100)	49/ 49(100)	7/ 7(100)	79/ 79(100)	22/ 22(100)
GFAP	0/10(0)	10/255(4.0)	0/57(0)	0/5(0)	0/68(0)	0/21(0)
NeuN	0/17(0)	9/207(4.3)	1/58(1.7)	1/ 6(16.7)	3/71(4.2)	0/22(0)

Number of cells double-positive for the apoptotic marker (either TUNEL or active caspase3) and the cell specific marker (CNPase, GFAP, or NeuN) per number of all cells positive for the apoptotic marker were shown. For example, in the TUNEL assay (left), 49 cells were found to be TUNEL-positive in EC and all of these 49 cells were also positive for CNPase (this does not mean that all CNPase-positive cells were also positive for TUNEL). Cells were counted in a total of 4 fields (100-fold magnification). Proportion of the cells positive for both TUNEL and cell-specific marker are shown in the parenthesis. Note that a large number of cells positive for TUNEL or caspase3 predominated in IC and EC. Most of them were double positive for CNPase and few were positive for GFAP or NeuN.

a: IC; internal capsule. b: EC; external capsule.

[9]. We examined 6 genes, namely *Grp78/Bip*, *Chop*, *Herpud1*, *Gadd45a*, *calnexin*, and *calreticulin* [13], in the IC by quantitative RT-PCR. We observed significant upregulation of all genes in *msd* mice with *Chop* showing the largest increase at P14 (Fig. 5), as previously reported [14,15]. However, curcumin treatment did not attenuate the expression of these genes.

Because a large number of oligodendrocytes undergoing apoptosis would be removed promptly from the *msd* brain, potentially concealing the attenuation effect of curcumin from detection *in vivo*, we also examined the same genes in a culture system using HeLa cells that transiently expressed mutant PLP1 to determine the direct effect of curcumin. Again, mutant PLP1 upregulated the expression of at least 4 out of 6 UPR genes (Fig S1A). However, curcumin treatment did not attenuate the expression of UPR genes (Fig S1B). These *in vivo* and *in vitro* findings suggest that the effect of curcumin may not be associated with UPR gene expression, at least in our experimental setting.

Next, we examined if curcumin changed the subcellular localization of accumulated mutant PLP1 proteins from the ER to the cytoplasm or plasma membrane, as observed in the CF and CMT1 studies [6–8]. HeLa cells were transiently transfected with a mutant *PLP1* plasmid and then examined by subcellular fractionation and western blotting (Figs. S2A and B). Mutant PLP1 showed only a faint signal in both fractions, which was not enhanced by curcumin treatment. In an immuno-cytochemistry study co-stained with an ER marker, calnexin, curcumin did not promote apparent translocation of the mutant PLP1 protein, while wild-type PLP1 appeared to show enhanced staining on cytoplasmic membrane after curcumin treatment (Fig. S2C).

4. Discussion

As therapeutic reagents for rare genetic disorders (especially in children), food compounds have considerable advantages with respect to safety, ethical issues, and material availability, as well as potential in clinical applications. In this study, we demonstrated that curcumin could serve as a potential therapeutic compound for PMD. Oral curcumin treatment extended the lifespan of *msd* mice by ~25% as compared to untreated mice. Although this extended survival was not accompanied by reconstitution of the CNS myelin and recovery in motor function, it inhibited apoptotic cell death in oligodendrocytes. As far as we know, curcumin represents the first compound that can mitigate the lethal phenotype caused by *PLP1* point mutations in the mouse. Because curcumin is a dietary compound with proven clinical safety in humans, it can be readily applied to patients with PMD that is caused by *PLP1* point mutations.

The exact mechanisms for the therapeutic action of curcumin were not fully elucidated. Curcumin has been reported to reduce oxidative damage, prevent amyloid formation, and decrease inflammation in the treatment of various neurodegenerative diseases and cancers by altering the activity of NF- κ B, AKT/mTOR, AP-1, NFR2, and protein kinases [16]. In addition, curcumin acts as an inhibitor of the sarco/endoplasmic reticulum Ca^{2+} ATPase (SERCA), presumably modifying ER stress [17]. Because the pathological processes of PMD involve not only protein misfolding and ER stress but also chronic inflammation [18,19], curcumin may elicit multifaceted pharmacological actions that work together to reduce oligodendrocyte cell death.

The modest therapeutic effects observed in *msd* mice contrasted with the dramatic improvement in the peripheral myelin in heterozygous *Tr-J* mice [8]. It is possible that curcumin may have limited therapeutic effects on genetically severe alleles. Massive apoptotic cell death of oligodendrocytes occurring at early postnatal stage would eliminate a major population of oligodendrocytes in *msd*. This would be more difficult to overcome than diseases with slower progression, like CF or CMT1. In fact, curcumin was not curative on the homozygous *Tr-J* allele, which causes a severe peripheral hypomyelination and death within a month (personal communication, M. Khajavi, JR Lupski). It is also possible that *msd* mutant PLP1 protein has stronger property to be stuck in ER than CFTR Δ 508 or PMP22 *Tr-J*, which are relatively milder disease alleles. In fact, curcumin may promote membrane trafficking of wild-type PLP1 (Fig. 7). Possibly, curcumin treatment on milder *PLP1* alleles may confer more obvious curative effects.

In conclusion, we demonstrated that a dietary compound, curcumin, is a potential therapeutic compound for patients with PMD carrying *PLP1* point mutations. As far as we know, this is the first study demonstrating such therapeutic effect on PMD *in vivo*. Because of its safety and wide applicability in humans, as evidenced in over 60 clinical trials [20], further evidence of the ability of curcumin to mitigate the PMD phenotype is awaited.

Acknowledgments

We thank Dr. W. B. Macklin (Cleveland Clinic Foundation, OH) for providing *msd* mice, Drs. I. Miyoshi, N. Yonemoto, and L. Goto (National Center for Neurology and Psychiatry, Japan) for their help in the statistical analyses, Dr. S. Yamashita (Kanagawa Children's Medical Center) for his advice in electron microscopic analysis and Harumi Iwashita and Eriko Arima for their technical assistance and animal care. This study was supported in part by grants from the Heath and Labour Sciences Research Grants, Research on Intractable Diseases (KI, H22-Nanchi-Ippan-132), Grants-in-Aid for Scientific Research from the Ministry of Education, Culture, Sports, Science and Technology, Japan (KI, 21390103 and 23659531), and a Grant from Takeda Science Foundation (KI).

Appendix A. Supplementary data

Supplementary data to this article can be found online at doi:10.1016/j.yimgme.2012.02.016.

References

- [1] K. Inoue, PLP1-related inherited dysmyelinating disorders: Pelizaeus–Merzbacher disease and spastic paraplegia type 2, *Neurogenetics* 6 (2005) 1–16.
- [2] J.Y. Garbern, Pelizaeus–Merzbacher disease: genetic and cellular pathogenesis, *Cell Mol. Life Sci.* 64 (2007) 50–65.
- [3] J. Garbern, F. Cambi, M. Shy, J. Kamholz, The molecular pathogenesis of Pelizaeus–Merzbacher disease, *Arch. Neurol.* 56 (1999) 1210–1214.
- [4] A. Gow, C.M. Southwood, R.A. Lazzarini, Disrupted proteolipid protein trafficking results in oligodendrocyte apoptosis in an animal model of Pelizaeus–Merzbacher disease, *J. Cell Biol.* 140 (1998) 925–934.
- [5] C.M. Southwood, J. Garbern, W. Jiang, A. Gow, The unfolded protein response modulates disease severity in Pelizaeus–Merzbacher disease, *Neuron* 36 (2002) 585–596.

- 374 [6] M.E. Egan, M. Pearson, S.A. Weiner, V. Rajendran, D. Rubin, J. Glockner-Pagel, S.
375 Canny, K. Du, G.L. Lukacs, M.J. Caplan, Curcumin, a major constituent of turmeric,
376 corrects cystic fibrosis defects, *Science* 304 (2004) 600–602.
- 377 [7] M. Khajavi, K. Inoue, W. Wiszniewski, T. Ohshima, G.J. Snipes, J.R. Lupski, Curcu-
378 min treatment abrogates endoplasmic reticulum retention and aggregation-
379 induced apoptosis associated with neuropathy-causing myelin protein zero-
380 truncating mutants, *Am. J. Hum. Genet.* 77 (2005) 841–850.
- 381 [8] M. Khajavi, K. Shiga, W. Wiszniewski, F. He, C.A. Shaw, J. Yan, T.G. Wensel, G.J.
382 Snipes, J.R. Lupski, Oral curcumin mitigates the clinical and neuropathologic phe-
383 notype of the Trembler-J mouse: a potential therapy for inherited neuropathy,
384 *Am. J. Hum. Genet.* 81 (2007) 438–453.
- 385 [9] V. Vasireddy, V.R. Chavali, V.T. Joseph, R. Kadam, J.H. Lin, J.A. Jamison, U.B. Kompella,
386 G.B. Reddy, R. Ayyagari, Rescue of photoreceptor degeneration by curcumin in trans-
387 genic rats with P23H rhodopsin mutation, *PLoS One* 6 (2011) e21193.
- 388 [10] S. Gencic, L.D. Hudson, Conservative amino acid substitution in the myelin pro-
389 teolipid protein of jimpy^{msd} mice, *J. Neurosci.* 10 (1990) 117–124.
- 390 [11] K. Kitamura, Y. Itou, M. Yanazawa, M. Ohsawa, R. Suzuki-Migishima, Y. Umeki, H.
391 Hohjoh, Y. Yanagawa, T. Shinba, M. Itoh, K. Nakamura, Y. Goto, Three human ARX
392 mutations cause the lissencephaly-like and mental retardation with epilepsy-like
393 pleiotropic phenotypes in mice, *Hum. Mol. Genet.* 18 (2009) 3708–3724.
- 394 [12] T. Morimura, M. Hattori, M. Ogawa, K. Mikoshiba, Disabled1 regulates the intra-
395 cellular trafficking of reelin receptors, *J. Biol. Chem.* 280 (2005) 16901–16908.
- 396 [13] I. Kim, W. Xu, J.C. Reed, Cell death and endoplasmic reticulum stress: disease rele-
vance and therapeutic opportunities, *Nat. Rev. Drug Discov.* 7 (2008) 1013–1030. 398
- [14] L.D. Hudson, N.L. Nadon, Amino acid substitutions in proteolipid protein that
cause dysmyelination, in: R.E. Martenson (Ed.), *Myelin: biology and chemistry*,
CRC press, Boca Raton, 1992, pp. 677–702. 400
- [15] C. Southwood, A. Gow, Molecular pathways of oligodendrocyte apoptosis
revealed by mutations in the proteolipid protein gene, *Microsc. Res. Tech.* 52
(2001) 700–708. 402
- [16] J.S. Jurenka, Anti-inflammatory properties of curcumin, a major constituent of
Curcuma longa: a review of preclinical and clinical research, *Altern. Med. Rev.*
14 (2009) 141–153. 404
- [17] J.G. Bilmen, S.Z. Khan, M.H. Javed, F. Michelangeli, Inhibition of the SERCA Ca²⁺
pumps by curcumin. Curcumin putatively stabilizes the interaction between the
nucleotide-binding and phosphorylation domains in the absence of ATP, *Eur. J.*
Biochem. 268 (2001) 6318–6327. 406
- [18] J.M. Edgar, M.C. McCulloch, P. Montague, A.M. Brown, S. Thilemann, L. Pratola, F.I.
Gruenenfelder, I.R. Griffiths, K.A. Nave, Demyelination and axonal preservation in
a transgenic mouse model of Pelizaeus–Merzbacher disease, *EMBO Mol. Med.* 2
(2010) 42–50. 408
- [19] C.L. Tatar, S. Appikatla, D.A. Bessert, A.S. Paintlia, I. Singh, R.P. Skoff, Increased *P1p1*
gene expression leads to massive microglial cell activation and inflammation
throughout the brain, *ASN Neuro* 2 (2010) art:e00043. 410
- [20] Curcumin Clinical Trials, <http://clinicaltrials.gov/ct2/results?term=curcumin>
[accessed January 11, 2012]. 412
- 420
421

422

